Square Kilometre Array - An overview

Raghunath Ghara
(NCRA-TIFR)

July 20, 2016

SKA1 SYSTEM BASELINEV2 DESCRIPTION

Document number	SKA-TEL-SKO-0000308
Context	AG-BD-RE
Revision	01
Author	Peter Dewdney
Date	2015-11-04
Document Classification	UNRESTRICTED
Status	Released

SKA1-LOW CONFIGURATION

Document number	SKA-SCI-LOW-001
Context	PPP-PPP-PPP-TTT
Revision	A
Author	SKAO Science Team
Date	2015-10-28
Document Classification	UNRESTRICTED
Status	Draft

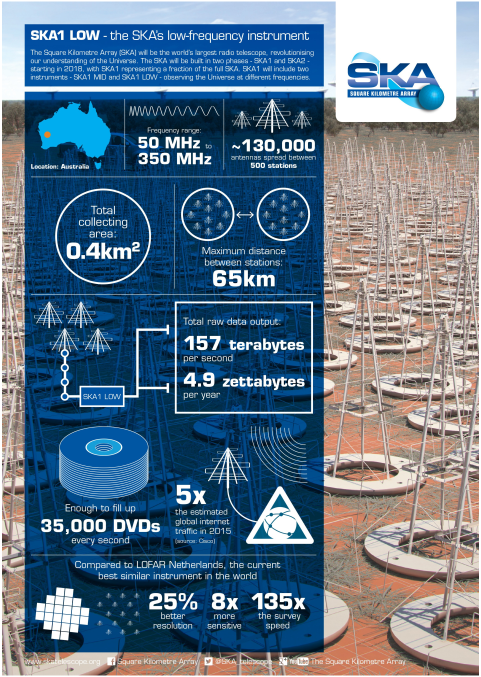

- **Main science goals :**
  - Cosmic dawn
  - Epoch of reionization
  - Pulsar timing low
  - Pulsar search low
- **Location :** Murchison Shire of Western Australia
- **Bandwidth :** 300 MHz (50 to 350 MHz frequency range)
- Will consist of an array of $\sim$130,000 dual-polarisation antenna elements.
- **Aperture array stations** (10s of metres in diameter): Antenna elements will be combined in groups so as to each act like single large antennas.

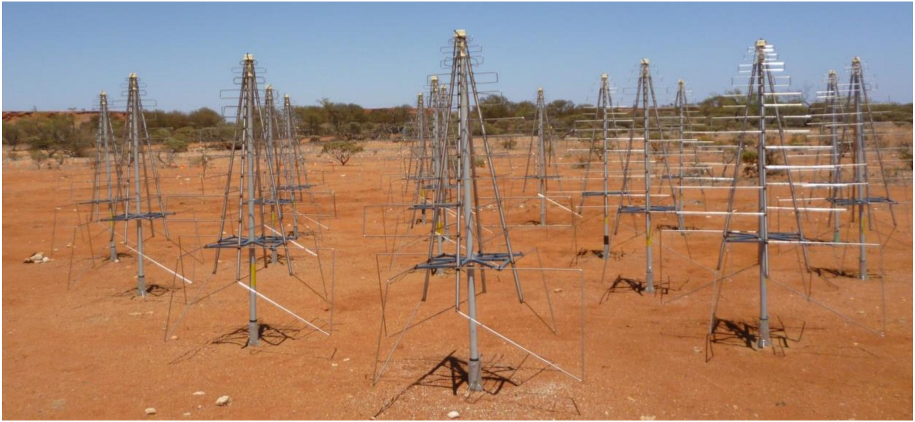

- Number of aperture array stations $\sim$ 564
- Capable of forming one or more 'beams' on the sky.
- Minimum/maximum separation between the stations: $\sim$ 30 m/65 km.
- FOV $\sim$ 20 deg^2.
- Long/short dipoles at the bottom/top cover the lowest/highest frequencies

SKA1-low antenna configuration

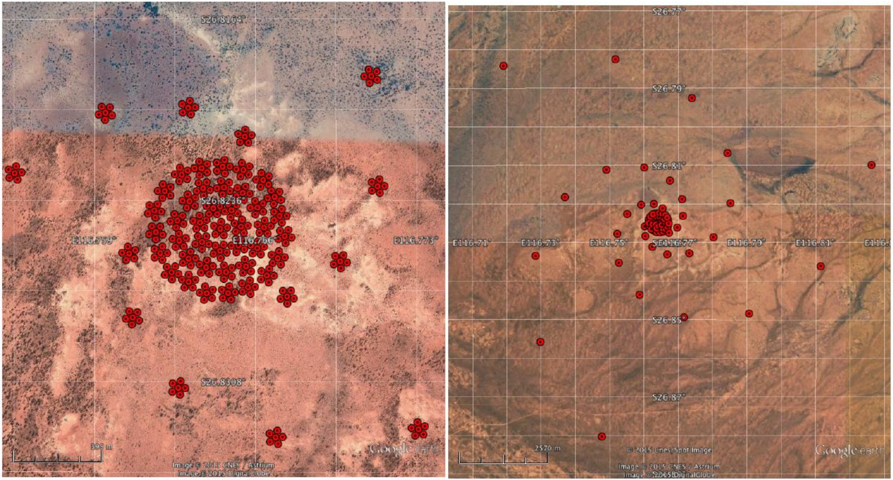

Figure 1: The SKA1-low core (left) and skirt (right). The tightly packed system of randomised concentric rings extends to a radius of about 350m. A tightly wound three arm logarithmic spiral extends between radii of 350m – 6400m.

SKA1-low UV coverage

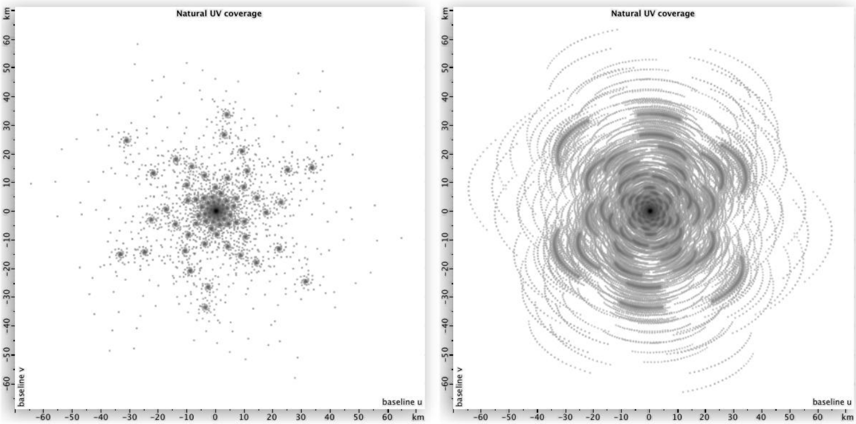

Figure 4: The SKA1-low snap-shot (left) and 4-hour tracking (right) visibility coverage for a monochromatic observation at a nominal declination of -30.

Sensitivity

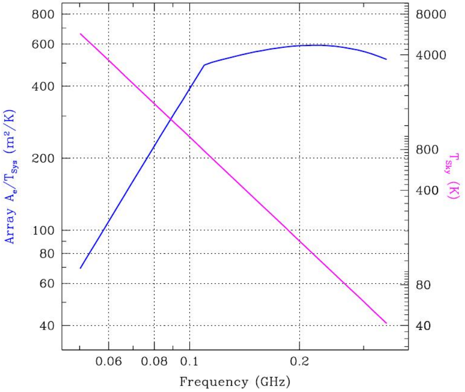

- System Temperature

  $$T_{\rm sys} \sim 60 \times (300~{\rm MHz}/\nu)^{2.55}~{\rm K}$$

- The sensitivity curve drops steeply below 110 MHz because the sky noise, which dominates the system temperature
- Above 110 MHz the increase of collecting area as λ^2 almost cancels the sky noise, and the ratio $(A_e/T_{\rm sys})$ is almost flat.

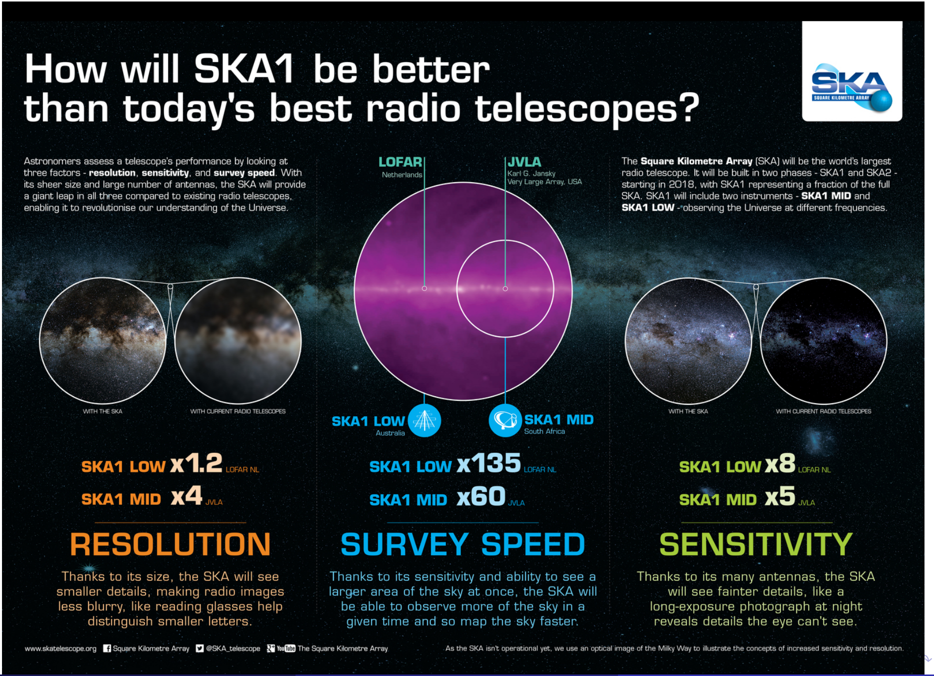
How will SKA1 be better than today's best radio telescopes?
SKA SQUARE KILOMETRE ARRAY
Astronomers assess a telescope's performance by looking at three factors - resolution, sensitivity, and survey speed. With its sheer size and large number of antennas, the SKA will provide a giant leap in all three compared to existing radio telescopes, enabling it to revolutionise our understanding of the Universe.
LOFAR
Netherlands
JVLA
Karl G. Jansky Very Large Array, USA
The Square Kilometre Array (SKA) will be the world's largest radio telescope. It will be built in two phases - SKA1 and SKA2 - starting in 2018, with SKA1 representing a fraction of the full SKA. SKA1 will include two instruments - SKA1 MID and SKA1 LOW - observing the Universe at different frequencies.
WITH THE SKA
WITH CURRENT RADIO TELESCOPES
SKA1 LOW
Australia
SKA1 MID
South Africa
WITH THE SKA
WITH CURRENT RADIO TELESCOPES
SKA1 LOW x1.2 LOFAR NL
SKA1 MID x4 JVLA
RESOLUTION
Thanks to its size, the SKA will see smaller details, making radio images less blurry, like reading glasses help distinguish smaller letters.
SKA1 LOW x135 LOFAR NL
SKA1 MID x60 JVLA
SURVEY SPEED
Thanks to its sensitivity and ability to see a larger area of the sky at once, the SKA will be able to observe more of the sky in a given time and so map the sky faster.
SKA1 LOW x8 LOFAR NL
SKA1 MID x5 JVLA
SENSITIVITY
Thanks to its many antennas, the SKA will see fainter details, like a long-exposure photograph at night reveals details the eye can't see.
www.skatelescope.org Square Kilometre Array @SKA_telescope The Square Kilometre Array
As the SKA isn't operational yet, we use an optical image of the Milky Way to illustrate the concepts of increased sensitivity and resolution.

Imaging the first sources during the cosmic dawn using SKA

Ghara R., Choudhury T. R., Datta K. K., Choudhuri S., arXiv:1607.02779

Motivation

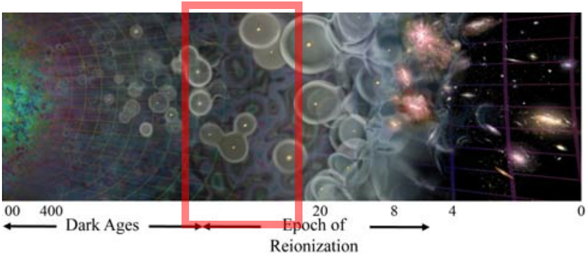

- Can we detect the first sources with radio interferometers like the SKA1-low? What informations can be obtained from that?
- IGM properties:
  - Neutral fraction
  - Kinetic temperature
- Source properties:
  - Mass of the source
  - Age
  - Escape fraction of UV photons $f_{\rm esc}$
  - UV and X-ray luminosity etc..

Differential brightness temperature ($\delta T_{\rm b}$)

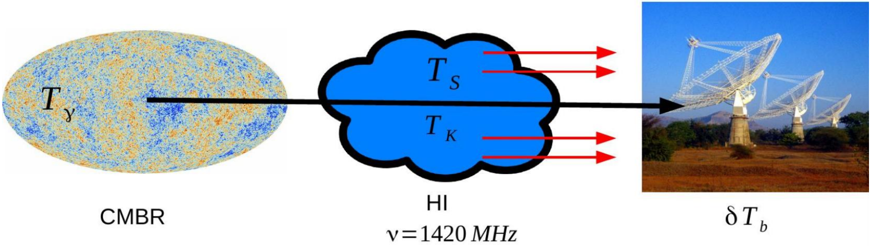

$$\delta T_{\rm b} = 27\ x_{\rm HI}\ (1+\delta_{\rm B}) \left(\frac{\Omega_{\rm B} h^2}{0.023}\right) \left(\frac{0.15}{\Omega_{\rm m} h^2}\frac{1+z}{10}\right)^{1/2} \left[1 - \frac{T_\gamma}{T_{\rm S}}\right]\ {\rm mK}$$

Differential brightness temperature ($\delta T_{\rm b}$)

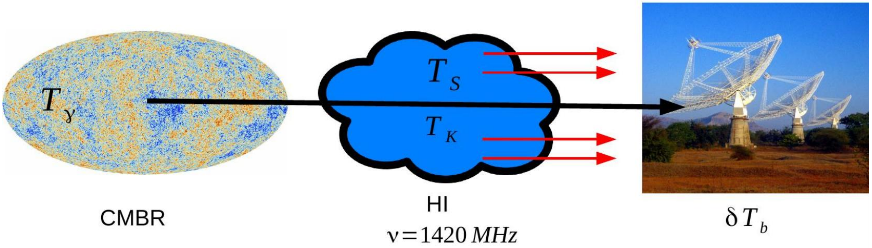

$$\delta T_{\rm b} = 27\, x_{\rm HI}\, (1+\delta_{\rm B}) \left(\frac{\Omega_{\rm B} h^2}{0.023}\right) \left(\frac{0.15}{\Omega_{\rm m} h^2}\frac{1+z}{10}\right)^{1/2} \left[1 - \frac{T_\gamma}{T_{\rm S}}\right] {\rm mK}$$

Density contrast

CMBR temperature

neutral fraction of hydrogen

Spin temperature

SKA1-low Baseline distribution

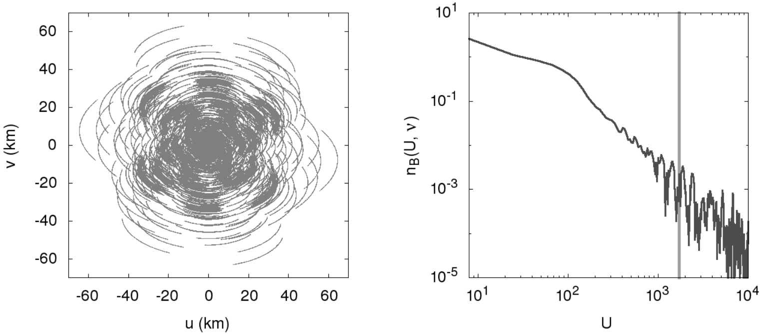

- Baseline $U = d/\lambda$. d is the distance between the antenna pair and λ observational wavelength.
- $n_{\rm B}(U, \nu)$ is the number of antenna pairs having same baseline U at frequency ν.

Possible sources: popIII stars, Galaxies, mini-QSO, HMXBs..

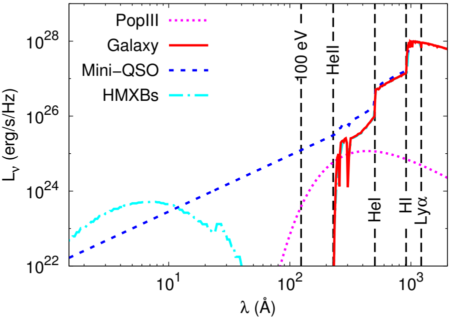

- $M_\star = 10^3\ \mathrm{M}_\odot$ for popIII
  $= 10^7\ \mathrm{M}_\odot$ for others.
- Spectral index $\alpha = 1.5$
- Ratio of X-ray and UV luminosity $f_X = 0.05$
- $f_{\rm esc} = 0.1$
- $t_{\rm age} = 20$ Myr

- The stellar part of the source is generated using PEGASE2 code : Salpeter IMF with 1-100 $\mathrm{M}_\odot$ population II stars, metallicity 0.001 $Z_\odot$.
- Mini-QSO : $I_q \propto E^{-\alpha}$, PopIII : black-body spectrum, HMXBs : absorption of soft-X-rays in ISM (Fragos et al 2013)

One-dimensional radiative transfer

- Inputs
  - SED : $\mathrm{Ly}\alpha$, UV, X-rays
  - An uniform background IGM
- Generate x_{HII} and T_{K} profile
  - Photo-ionization, Collisional ionization, Recombinations
  - Photoelectric heating, Compton heating, cooling due to collisional excitation, Hubble expansion etc.
- Assume $\mathrm{Ly}\alpha$ photon flux reduces as $1/R^2$ with radial distance R.
- Calculate the coupling coefficients and spin temperature (T_{S}) profile.
- Use x_{HII} and T_{S} profiles to generate δT_{b} profile.

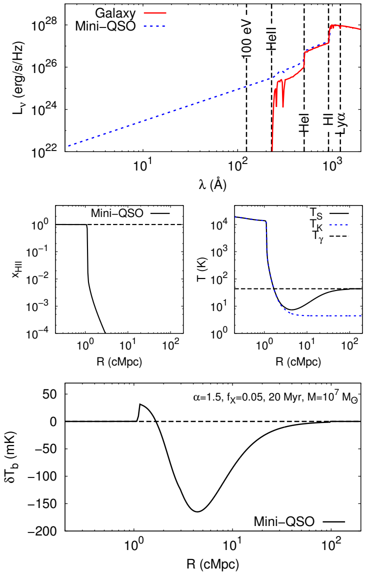

δT_b profiles

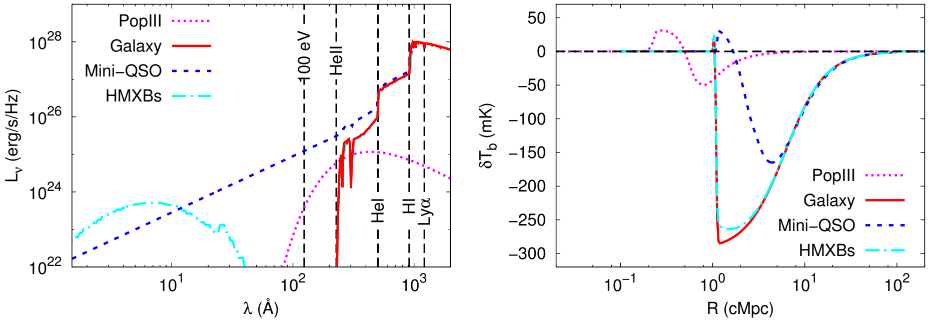

- Signals are different around different type of sources. Redshift = 15

$\delta T_{\rm b}$ profiles

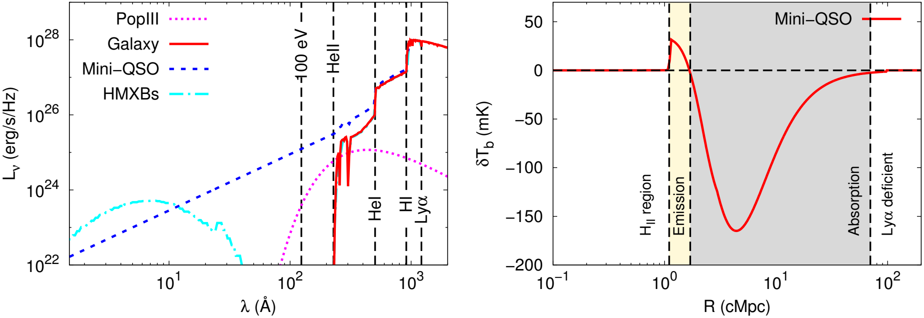

- Signals are different around different type of sources. Redshift = 15
- $\delta T_{\rm b}$ pattern around a source :
    - H II region at the center ($\delta T_{\rm b} = 0$),
    - Emission region ($\delta T_{\rm b} > 0$),
    - Absorption region ($\delta T_{\rm b} < 0$),
    - Lyα deficient region ($\delta T_{\rm b} \sim 0$).

Isolated source : simple Model

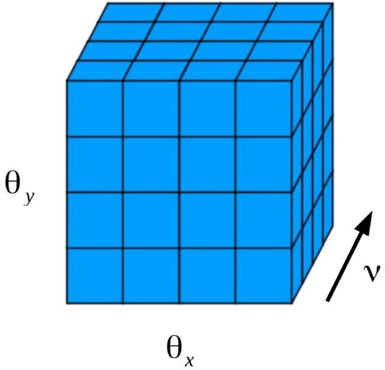

- The angular extent of the simulation box is determined by the minimum baseline.
- The angular resolution is determined by the maximum baseline.
- Length of the box along the frequency direction is determined by the observational band width.
- We assume that the source is at the center of the simulation box.
- We will image the central frequency channel.

Signal simulation

- Differential brightness temperature :

$$\delta T_{\rm b}(\vec{\theta}, \nu) \propto x_{\rm HI}(\mathbf{x}, z)[1 + \delta_{\rm B}(\mathbf{x}, z)] \left[1 - \frac{T_\gamma(z)}{T_{\rm S}(\mathbf{x}, z)}\right]$$

- Sky specific intensity :

$$I_\nu(\vec{\theta}) = \frac{2k_B\nu^2}{c^2}\delta T_{\rm b}(\vec{\theta}, \nu)$$

- Flux per synthesised beam :

$$S_\nu = I_\nu(\vec{\theta}) \times \Delta\Omega,$$

where $\Delta\Omega = (\Delta\theta)^2$ is the beam solid angle.

- Dirty image : We first obtain the visibilities of the signal at each *uv* grid point and then multiply the signal with the baseline (*uv*) sampling function.

Noise simulation

- The system noise at different baselines and frequency channels are expected to be Gaussian random variables with zero mean.
- rms noise :

$$\sqrt{\langle N^2 \rangle} = \frac{\sqrt{2} k_B T_{\rm sys}}{A_{\rm eff} \sqrt{\Delta \nu_c \ \Delta t_c}} \tag{1}$$

- Pixel noise can be reduced using long observation time.
- Also by a factor $1/\sqrt{n^{i,j}_{\rm Base}}$, where $n^{i,j}_{\rm Base}$ is the number of antenna pairs associated with the i,j th pixel.
- Reduction factor : $\sqrt{t_{\rm obs}/t^{uv}_{\rm obs}}$, $t^{uv}_{\rm obs} = 4$ h
- Reverse Fourier transform to get noise maps in real space.

Simulated signal and noise

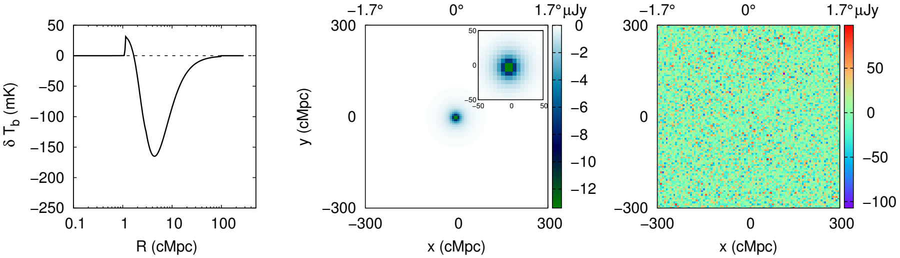

- Fiducial source : $M_\star = 10^7\ \mathrm{M_\odot}$, Spectral index $\alpha = 1.5$, ratio of X-ray and UV luminosity $f_X = 0.05$, $f_{\rm esc} = 0.1$, $t_{\rm age} = 20\ \mathrm{Myr}$,
- Angular resolution : $2'$
- Noise map correspond to an observation time of 2000 h and frequency resolution of 100 kHz.

Smoothed maps (Foregrounds free)

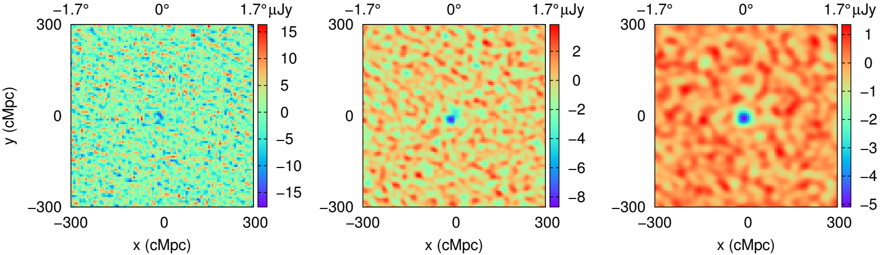

- Angular resolution : $2'$
- Observational time : 2000 h, frequency resolution : 100 kHz
- Gaussian filter of size $10'$ (left), $20'$ (middle), $30'$ (right).
- SNRs : 4 (left), 7.5 (middle), 11 (right)

Parameter estimation?

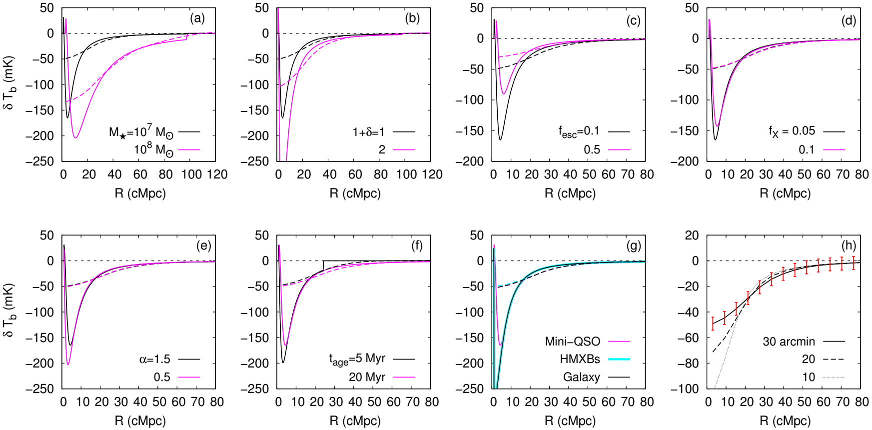

- Fiducial source : Mini-QSO ($M_\star = 10^7\ \mathrm{M}_\odot$, $\alpha = 1.5$, $f_X = 0.05$, $f_{\rm esc} = 0.1$, $t_{\rm age} = 20\ \mathrm{Myr}$)
- Angular resolution : $2'$, Gaussian filter : $30'$

Signal to noise ratio

Source	$M_\star$	$1+\delta$	$f_{\rm esc}$	$1+z$	Filter	SNR1	SNR2
Mini-QSO	$10^7 {\rm M}_\odot$	1	0.1	16	$30'$	11.1	9.1
Mini-QSO	$10^6 {\rm M}_\odot$	1	0.1	16	$30'$	3.6	3.4
Mini-QSO	$10^8 {\rm M}_\odot$	1	0.1	16	$30'$	25.9	20.2
Mini-QSO	$10^7 {\rm M}_\odot$	2	0.1	16	$30'$	20.4	17.5
Mini-QSO	$10^7 {\rm M}_\odot$	1	0.5	16	$30'$	5.2	4
Mini-QSO	$10^7 {\rm M}_\odot$	1	0.1	11	$30'$	46	38
Mini-QSO	$10^7 {\rm M}_\odot$	1	0.1	16	$10'$	4.2	4.0
Galaxy	$10^7 {\rm M}_\odot$	1	0.1	16	$30'$	11.3	9.4
HMXBs	$10^7 {\rm M}_\odot$	1	0.1	16	$30'$	11.2	9.2

- $t_{\rm obs}$ =2000 h, $\Delta\nu$ =100 kHz
- SNR1 : without foregrounds
- SNR2 : with foregrounds

Foregrounds?

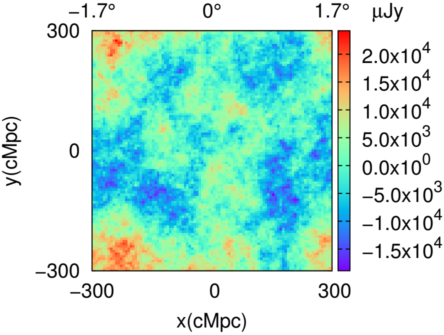

- Galactic Synchrotron radiation
- Unresolved extragalactic point sources

Foregrounds?

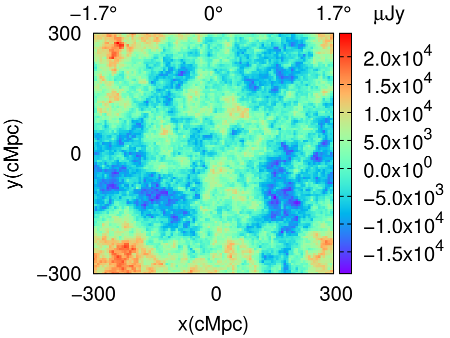

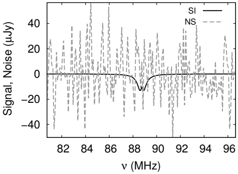

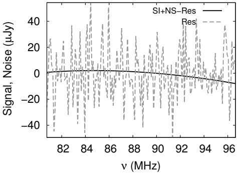

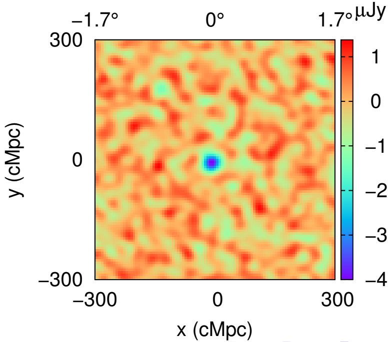

- Galactic Synchrotron radiation
- Unresolved extragalactic point sources

- SNR $\sim$ 9

Using a filter

- Signal estimator:

$$\left\langle \hat{E} \right\rangle = \int \mathrm{d}^2 U \int \mathrm{d}\nu \; S(\vec{U}, \nu) \; S_f^{\star}(\vec{U}, \nu) \; n_{\mathrm{B}}(\vec{U}, \nu)$$

- Noise :

$$\left\langle (\Delta \hat{E})^2 \right\rangle_{\mathrm{NS}} = A_{\mathrm{NS}} \int \mathrm{d}^2 U \int \mathrm{d}\nu \; |S_f(\vec{U}, \nu)|^2 \; n_{\mathrm{B}}(\vec{U}, \nu)$$

where,

$$A_{\mathrm{NS}} = \left\langle \hat{N}^2 \right\rangle \frac{2}{N_{\mathrm{ant}}(N_{\mathrm{ant}} - 1)} \frac{\Delta \nu_c}{B_\nu}$$

- Foregrounds : (Datta et al 2007)

$$\left\langle (\Delta \hat{E})^2 \right\rangle_{\mathrm{FG}} = \int \mathrm{d}^2 U \int \mathrm{d}\nu_1 \int \mathrm{d}\nu_2 \left(\frac{2K_B}{c^2} \right)^2 (\nu_1 \nu_2)^2$$
$$\times \; n_{\mathrm{B}}(\vec{U}, \nu_1) \; n_{\mathrm{B}}(\vec{U}, \nu_2) \; C_{2\pi U}(\nu_1, \nu_2)$$
$$\times \; S_f^{\star}(\vec{U}, \nu_1) S_f(\vec{U}, \nu_2)$$

Using a filter

- Filter :

$$S_f(\vec{U},\nu) = \left(\frac{\nu}{\nu_c}\right)^2 [S_T(\vec{U},\nu,B_f) - \frac{\Theta(1-|\nu-\nu_c|/B^{'})}{B^{'}} \times \int_{\nu_c-B^{'}/2}^{\nu_c+B^{'}/2} S_T(\vec{U},\nu^{'},B_f)\ d\nu^{'}]$$

with $B^{'} = 2B_f$ if $B^{'}$ is less than B_ν, else $B^{'} = B_\nu$.

$$S_T(\vec{U},\nu,B_f) = 0 \text{ if } |\nu-\nu_c| > \frac{B_f}{2}$$
$$= -1 \text{ if } |\nu-\nu_c| \leq \frac{B_f}{2}.$$

Using a filter

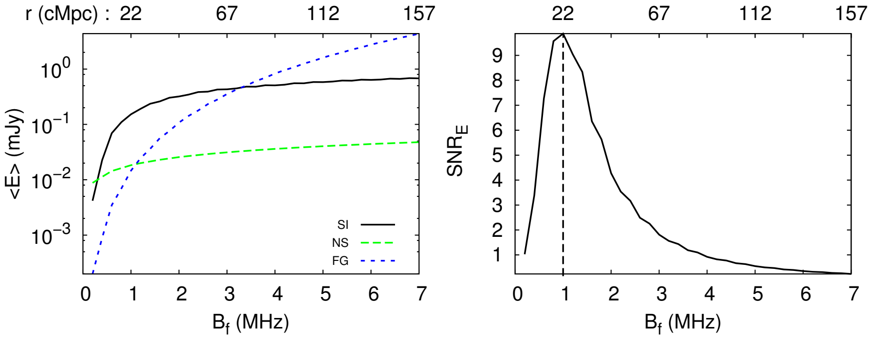

Realistic scenario : Semi-numerical model

- Dark matter Simulation:
  - Cosmological $N-$body code : CUBEP^{3}M (Harnois-Deraps et al. 2012)

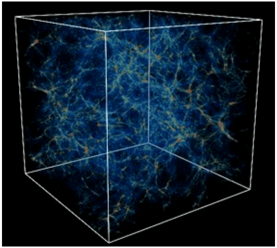

Realistic scenario : Semi-numerical model

- Dark matter Simulation:
  - Cosmological $N-$body code : CUBEP^{3}M (Harnois-Deraps et al. 2012)
- Identify Dark matter haloes.

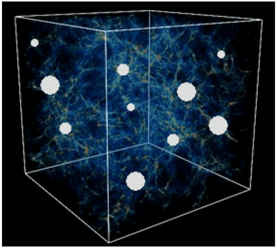

Realistic scenario : Semi-numerical model

- Dark matter Simulation:
  - Cosmological $N-$body code : CUBEP^{3}M (Harnois-Deraps et al. 2012)
- Identify Dark matter haloes.
- These haloes are embedded with the sources of radiation.

$$M_\star = f_\star \left(\frac{\Omega_B}{\Omega_m}\right) M_{\rm halo}$$

$f_\star$ is the stellar fraction of the baryon in the source.

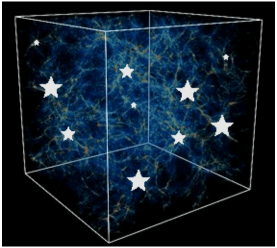

Realistic scenario : Semi-numerical model

- Dark matter Simulation:
  - Cosmological $N-$body code : CUBEP^{3}M (Harnois-Deraps et al. 2012)
- Identify Dark matter haloes.
- These haloes are embedded with the sources of radiation.

$$M_\star = f_\star \left(\frac{\Omega_B}{\Omega_m}\right) M_{\rm halo}$$

$f_\star$ is the stellar fraction of the baryon in the source.

- Radial profile of ionization fraction and temperature is derived using a 1D radiative transfer code.

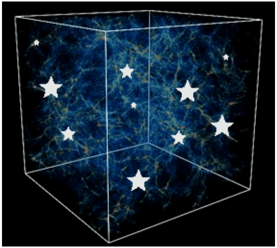

Realistic simulation : Signal maps

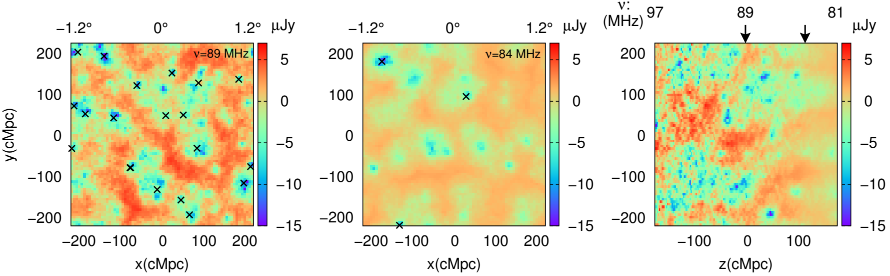

- '×' marks: θ_x, θ_y positions of the sources.
- Simulation :
  - simulation box of size 300 h^{-1} cMpc
  - 2592^3 particles
  - The minimum halo identified using spherical overdensity method is $\sim 4 \times 10^9\ \mathrm{M}_\odot$.
- Mean is subtracted at each frequency channel.

Realistic maps : Foregrounds subtracted and smoothed

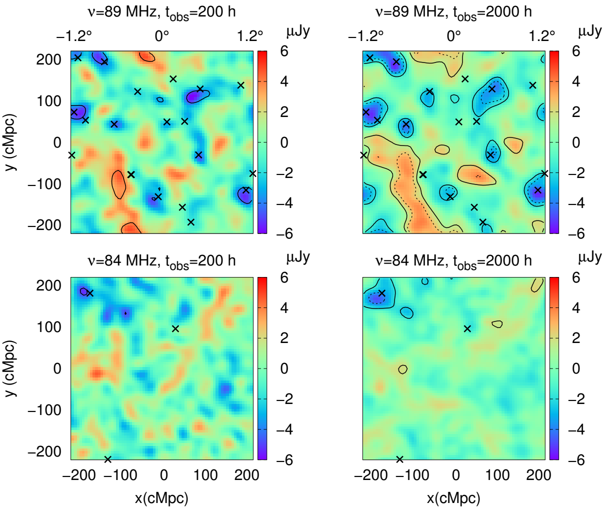

- SNR : Upper panels (4.8, 14.2), Lower panels (3.3, 10)
- **One possible observational strategy:** observe multiple fields, detect the signal in low resolution images for short $t_{\rm obs}$, longer observation on the field where signal is detected, recover the $\delta T_{\rm b}$ profiles, parameter estimation.

Conclusions

- After subtracting the foreground sufficiently and suppressing the rms noise by smoothing using a Gaussian filter, the sources are detectable with $\sim 9 - \sigma$ confidence level over 2000 hours of observation with the SKA1-low in images of resolution $2'$.
- Although the 21-cm profiles around the sources get altered because of the Gaussian smoothing, the images can still be used to extract some of the source properties.
- Possible to suppress the foregrounds contributions and detect the signal using suitable filters.
- These studies are useful for making observational strategies.